J|A|C|S
ARTICLES
Published on Web 11/01/2002

Ambident Ethyl *N*-Nitrosocarbamate Anion: Experimental and Computational Studies of Alkylation and Thermal Stability

Vladimir Benin,[†,‡] Piotr Kaszynski,*[,†] and J. George Radziszewski[§]

Contribution from the Organic Materials Research Group Department of Chemistry, Vanderbilt University, Nashville, Tennessee 37235, Department of Chemistry, Colorado School of Mines, Golden, Colorado, 80401, and National Renewable Energy Laboratory, Golden, Colorado 80401

Received July 1, 2002. Revised Manuscript Received August 22, 2002

Abstract: Alkylation of *N*-nitrosourethane tetrabutylammonium salt (**2-Bu$_4$N**) with four electrophiles (MeI, EtI, *i*-PrI, and PhCH$_2$Br) was studied by ^{1}H NMR in CD_2Cl_2 and CD_3CN solutions. The ratio of the three regioisomers *N*-alkyl-*N*-nitrosourethane **3**, azoxy **4**, and *O*-alkyldiazotate **5** was practically independent of solvent but dependent on the nature of the electrophile. The anion **2** and *O*-alkyl derivative **5** are thermally unstable and decompose to ethyl carbonates **9** and **10**, respectively, with a first-order rate constant (**2-Bu$_4$N**: $k = 18.5 \pm 0.1 \times 10^{-5}$ s^{-1}; **5b** (R = Et): $k = 1.77 \pm 0.02 \times 10^{-5}$ s^{-1}; **5d** (R = PhCH$_2$): $k = 4.78 \pm 0.08 \times 10^{-5}$ s^{-1} at 35 °C in CD_2Cl_2). Further kinetic measurements gave activation parameters for the decomposition of **2** ($E_a = 24.2 \pm 0.3$ kcal/mol and ln $A = 30.9 \pm 0.1$). Gas-phase calculations at the MP2(fc)/6-31+G(d)//MP2(fc)/6-31G(d) level showed that the alkylation of **2** involves the lone electron pairs of the N−N−O atoms, and the calculated activation energies correspond well to the observed ratio of regioisomers **3**−**5**. The theoretical analysis of the decomposition processes supports a concerted mechanism with a four-center transition state in the first step for all four compounds. The calculated activation energy order (**2** < **5** < **3** < **4**) is consistent with the observed order of stability. Decomposition of **2** and **5** is a unimolecular process, giving carbonates **9** and **10** in a single step. In contrast, rearrangement of **3** and **4** leads to alkyl diazonium ions. A detailed theoretical analysis indicates that the rate-determining step for thermal decomposition of **2** is the loss of molecular nitrogen, while in **5** it is the trans−cis isomerization process. The nonconcerted process involving homolytic cleavage of the O−N bond in **5** was found to be significantly less favorable.

Introduction

N-nitrosoamides, *N*-nitrosocarbamates, and *N*-nitrosoureas are of considerable interest in synthetic chemistry, biochemistry, and medicine. They have been used as reagents,[1−4] studied for their mutagenic and cancerogenic properties,[5] and suggested as antitumor agents.[6] Most of these studies have focused on the *N*-alkyl-*N*-nitroso derivatives, while much less attention has been paid to the properties and chemistry of secondary *N*-nitroso derivatives. Such compounds are generally less stable than the *N*-alkyl analogues but are formed equally easily from the −CONH$_2$ derivatives under mild nitrosylation conditions.[4] Unlike the tertiary *N*-alkyl derivatives, however, the secondary *N*-nitrosoamides easily dissociate in aqueous solutions to form ambident anions.[7] Surprisingly, the chemistry of such anions and their reactions with electrophiles has received little attention.

During the past century, only a handful of secondary *N*-nitrosoamides have been isolated and investigated. Perhaps the best studied among them is *N*-nitrosourethane **1**.[8] It has been established that **1** is more acidic than acetic acid,[9] dissociates to form the anion **2**, has limited stability in water and in the presence of amines,[8,10] and forms a stable Pd complex.[11] With the exception of a report[9] on the formation of a silver salt **2-Ag** and its reaction with MeI, no further investigations of **1** or its anion **2** have been documented.

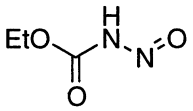

1

Anion **2** belongs to a relatively broad class of diazotates (anions derived from monosubstituted *N*-nitrosoamines), most

* Author for correspondence. Phone: (615)322-3458; fax: (615)343-1234; e-mail: PIOTR@ctrvax.vanderbilt.edu.
† Vanderbilt University.
‡ Present address: Department of Chemistry, University of Dayton, 300 College Park, Dayton, OH 45469-2357.
§ Colorado School of Mines and National Renewable Energy Laboratory.

(1) White, E. H. *J. Am. Chem. Soc.* **1955**, *77*, 6011−6014.
(2) Godfrey, A. G.; Ganem, B. *J. Am. Chem. Soc.* **1990**, *112*, 3717−3718.
(3) Regitz, M.; Maas, G. *Diazo Compounds*; Academic Press: New York, 1986; Chapter 12, pp 301−325.
(4) (a) Collet, H.; Bied, C.; Mion, L.; Taillades, J.; Commeyras, A. *Tetrahedron Lett.* **1996**, *37*, 9043−9046. (b) Collet, H.; Boiteau, L.; Taillades, J.; Commeyras, A. *Tetrahedron Lett.* **1999**, *40*, 3355−3358.
(5) Selected general references: (a) *Nitrosamines and Related N-Nitroso Compounds: Chemistry and Biochemistry*; Loeppky, R. N., Michejda, C. J., Eds.; American Chemical Society: Washington, DC, 1994; Vol. 553. (b) *Nitrosamines: Toxicology and Microbiology*; Hill, M. J., Ed.; VCH: Chichester, England, 1988. (c) *N-Nitroso Compounds*; Scanlan, R. A., Tannenbaum, S. R., Eds.; American Chemical Society: Washington, DC, 1981; Vol. 174. (d) *N-Nitrosamines*; Anselme, J.-P., Ed.; American Chemical Society: Washington, DC, 1979; Vol. 101. (e) Digenis, G. A.; Issidorides, C. H. *Bioorg. Chem.* **1979**, *8*, 97−137, and references therein.
(6) Gnewuch, C. T.; Sosnovsky, G. *Chem. Rev.* **1997**, *97*, 829−1013.
(7) Reutov, O. A.; Beletskaya, I. P.; Kurts, A. L. *Ambident Anions*; Consultants Bureau: New York, 1983.
(8) Thiele, J.; Lachman, A. *Justus Liebigs Ann. Chem.* **1895**, *288*, 267−311.

Scheme 1

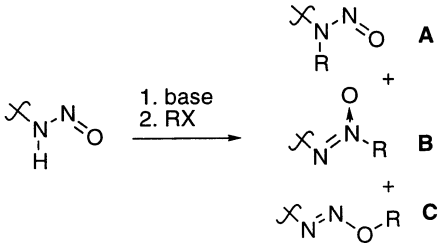

of which bear either an alkyl or an aryl substituent. Alkylation of these ambident anions is known to yield three possible products (Scheme 1) whose formation depends on the reaction conditions and the structure of the reactants. Generally, alkanediazotates react with alkyl electrophiles to yield the N-alkylated derivatives **A**.[12,13] However, under highly polar aprotic conditions the corresponding azoxy compounds **B** were isolated in good yields,[14,15] and the formation of significant quantities of unstable *O*-alkyl products **C** has been postulated.[16] When a diazotate carries an aryl substituent, alkylation yields a mixture of isolable N- and O-alkylated products, **A** and **C**, but no formation of the azoxy regioisomer **B** has been reported.[17,18] It has been demonstrated that the preference for O-alkylation increases in polar aprotic solvents and for more bulky alkyl halides.[17,18] The exclusive formation of the O-alkylated product **C** has been reported for some *N*-aryl-[19−22] and *N*-ethoxycarbonyldiazotates[9] carrying the Ag^+ cation,[23,24] which promotes an S_N1-type reaction and readily coordinates with the N-center.[25] Simultaneous formation of all three regioisomers has never been observed directly in any of the diazotates.

Despite the numerous experimental results, there is no reported computational analysis for the alkylation of diazotates. This is in contrast with enolates, carbon analogues of diazotates, whose regiochemistry of alkylation and thermodynamic stability has been extensively studied experimentally[7,26−28] and computationally.[29−31] To our knowledge, there is also no theoretical work on the thermal decomposition of *N*-nitrosoamides or related compounds. This is particularly surprising since an enormous body of work involving mechanistic and carcinogenic studies of these compounds has accumulated over the past half a century.

Scheme 2

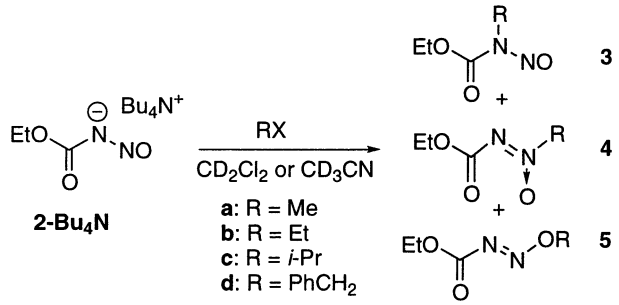

Scheme 3

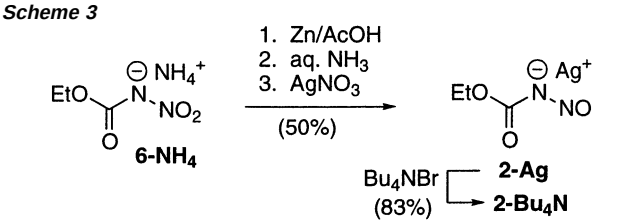

Scheme 4

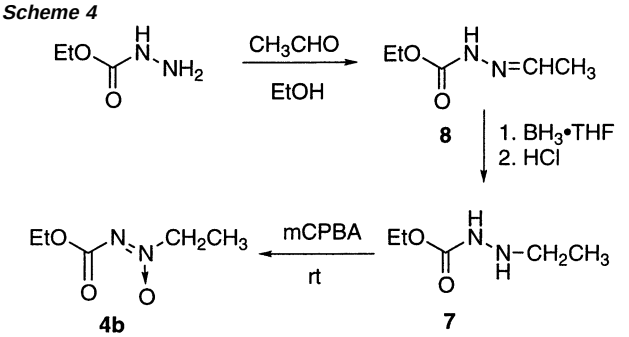

Here we examine the alkylation of tetrabutylammonium ethoxycarbonyldiazotate (**2-Bu$_4$N**) with three alkyl iodides and benzyl bromide in aprotic solvents and study the formation of the three regioisomeric products **3**−**5** as a function of solvent polarity and steric demands of the electrophile (Scheme 2). The discussion of the observed regiochemistry of alkylation and thermal stabilities of anion **2** and products **3**−**5** is aided with extensive quantum-mechanical calculations of ground and transition state structures.

Results

Synthesis. *N*-Nitrosourethane (**1**) was prepared according to a literature procedure[8] by partial reduction of *N*-nitrourethane (**6**).[32] The relatively unstable **1** was isolated as the silver salt **2-Ag**,[8] which was converted to the tetrabutylammonium salt **2-Bu$_4$N** (Scheme 3).

Azoxy ester **4b** was prepared by oxidation of ethyl 2-ethylcarbazate (**7**) with *m*-chloroperbenzoic acid (mCPBA, Scheme 4). The ethylcarbazate **7** was obtained by borane reduction of ethyl 2-ethylidenecarbazate (**8**) according to a general procedure.[33] Direct ethylation of ethyl carbazate with ethyl iodide or MeCHO/NaCN•BH_3 in EtOH gave largely the diethyl derivative.

(9) Hantzsch, A.; Schümann, M.; Engler, A. *Chem. Ber.* **1899**, *32*, 1703−1716.
(10) (a) Thiele, J.; Dent, F. *Justus Liebigs Ann. Chem.* **1898**, *302*, 245−272. (b) Pechman, v. H. *Chem. Ber.* **1898**, *31*, 2640.
(11) Robson, R. *Inorg. Chim. Acta* **1984**, *85*, 195−198.
(12) Schraube, C.; Schmidt, C. *Chem. Ber.* **1894**, *27*, 514−523.
(13) Keefer, L. K.; Wang, S.; Anjo, T.; Fanning, J. C.; Day, C. S. *J. Am. Chem. Soc.* **1988**, *110*, 2800−2806.
(14) Moss, R. A.; Landon, M. J.; Luchter, K. M.; Mamantov, A. *J. Am. Chem. Soc.* **1972**, *94*, 4392−4394.
(15) Cooper, C. S.; Peyton, A. L.; Weinkam, R. J. *J. Org. Chem.* **1983**, *48*, 4116−4119.
(16) Moss, R. A. *Acc. Chem. Res.* **1974**, *7*, 421−427.
(17) Voropaeva, A. P.; Gladysheva, L. M.; Ketlinskii, V. A.; Bagal, I. L.; Bryuske, Y. E.; Eltsov, A. V. *J. Org. Chem. USSR* **1974**, *12*, 395−404.
(18) Kozminski, W.; Jazwinski, J.; Stefaniak, L. *Magn. Reson. Chem.* **1993**, *31*, 200−202.
(19) Bamberger, E. *Chem. Ber.* **1895**, *28*, 225−244.
(20) Pechmann, v. H.; Frobenius, L. *Chem. Ber.* **1894**, *27*, 672−3.
(21) Masoud, N. K.; Ishak, M. F. *J. Chem. Soc., Perkin Trans. 2* **1988**, 927−931.
(22) Stepanov, S. D.; Pevzner, M. S.; Temchenko, T. P. *J. Org. Chem. USSR* **1989**, *24*, 1935−1940.
(23) Wulfman, D. S. In *The Chemistry of Diazonium and Diazo Groups*; Patai, S., Ed.; Wiley & Sons: New York, 1978; Vol. 1, pp 247−338.
(24) Zollinger, H. *Diazo Chemistry I*; VCH: New York, 1994; Vol. 1, p 109.
(25) Kornblum, N.; Smiley, R. A.; Blackwood, R. K.; Iffland, D. C. *J. Am. Chem. Soc.* **1955**, *77*, 6269−6280.
(26) Pollack, R. M. *Tetrahedron* **1989**, *45*, 4913−4938.
(27) Brickhouse, M. D.; Squires, R. R. *J. Phys. Org. Chem.* **1989**, *2*, 389−409.
(28) Jones, M. E.; Kass, S. R.; Filley, J.; Barkley, R. M.; Ellison, G. B. *J. Am. Chem. Soc.* **1985**, *107*, 109−115.
(29) Houk, K. N.; Paddon-Row, M. N. *J. Am. Chem. Soc.* **1986**, *108*, 2659−2662.
(30) Marcos, E. S.; Bertran, J. *J. Chem. Soc., Faraday Trans. 2* **1989**, *85*, 1531−1538.
(31) Lee, I.; Park, H. Y.; Han, I.-S.; Kim, C. K.; Kim, C. K.; Lee, B.-S. *Bull. Korean Chem. Soc.* **1999**, *20*, 559−566.
(32) Luk'yanov, O. A.; Kozlova, I. K.; Shitov, O. P.; Konnova, Y. V.; Kalinina, I. V.; Tartakovsky, V. A. *Russ. Chem. Bull.* **1996**, *45*, 863−867.
(33) Ghali, N. I.; Venton, D. L.; Hung, S. C.; Le Breton, G. C. *J. Org. Chem.* **1981**, *46*, 5413−5414.

Reactions of 2-Bu$_4$N with Alkyl Halides. Reactions of tetrabutylammonium salt **2-Bu$_4$N** with several alkyl iodides were conducted in two solvents of different polarity, CD_2Cl_2 and CD_3CN, at 0 °C or ambient temperature. The progress of the reactions and the rate of formation of products (Scheme 2) were monitored by ^{1}H NMR. In all cases the A_3X_2 signal for the ethyl group of the starting material **2-Bu$_4$N** and the characteristic signals for the alkyl halides were observed to diminish with a concomitant appearance of new, downfield-shifted sets of signals for the products. Reactions of **2-Bu$_4$N** with methyl iodide and benzyl bromide, run at 0 °C, resulted in three clean sets of NMR signals. Analogous reactions with ethyl and isopropyl iodides were conducted at ambient temperature and resulted in a mixture of at least five compounds. NMR analysis revealed that two identical sets of A_3X_2 signals (δ 1.10 (t), 1.14 (t), 3.58 (q), 3.77 (q) in CD_2Cl_2 and δ 1.06 (t), 1.09 (t), 3.51 (q), 3.70 (q) in CD_3CN) were present in the spectra of the reaction mixtures. The relative intensity of the common signals was significantly lower for the reaction of **2-Bu$_4$N** with ethyl than with isopropyl iodide. For reactions with isobutyl iodide the common signals were the major feature in the spectrum of the crude reaction mixture. These additional signals were assigned to products of the thermal decomposition of the starting salt **2-Bu$_4$N** (vide infra). An example of the NMR spectrum is shown in Figure 1a for the reaction of **2-Bu$_4$N** with ethyl iodide.

The NMR signals (Table 1) were assigned to the three products shown in Scheme 2 based on matching intensities and coupling constants, general spectroscopic trends, literature reports for some derivatives **3**,[15,34] an authentic sample of **4b**, and differential thermal stability. Thus, the signals of the α-hydrogens of the alkyl substituents in *N*-alkyl-*N*-nitrosocarbamates **3** are in the region between 3.1 (**3a**, R = Me) and 4.88 (**3d**, R = CH_2Ph) ppm and are upfield-shifted from the signals belonging to the two other isomers by about 0.4 (**3c**, R = *i*-Pr) to 1.0 (**3a**, R = Me) ppm.

The signals for the two other regioisomers, **4** and **5**, appear close together in the range characteristic for alkyl esters. Azoxy derivative **4b** was unambiguously identified in the reaction mixture of **2-Bu$_4$N** with ethyl iodide by comparison of the NMR spectrum with that of an authentic sample. Also, the NMR signal of the methyl group in the azoxy derivative **4a** is similar to that in its amide analogue, lyophyllin.[35] The remaining low field NMR signals of crude reaction mixtures were assigned to the O−CH_2− group in **5** and are consistent with those reported for their close aryl analogues.[36]

Further support for the assignments in Table 1 is provided by the difference in thermal stability of regioisomers **4** and **5**. The reaction mixtures prepared in CH_2Cl_2 were passed through a silica gel plug to remove the ammonium salts, redissolved in CD_2Cl_2, and thermolyzed at 35 °C for about 7 h. The low field set of signals that disappeared from the spectrum was assigned to the O-alkylated product **5**, while the remaining low field set belongs to the azoxy regioisomer **4**. This is shown for the ethylation reaction mixture in Figure 1. Further thermolysis of the crude mixture at 80 °C for 1 h resulted in the complete disappearance of the signals attributed to **4**, and the only remaining set of signals was that belonging to *N*-alkyl isomer **3**. The complete assignments are shown in Table 1.

The yields for the alkylation reactions were obtained by comparing the total intensities of the −COO**CH$_2$**CH$_3$ signals in the three regioisomers with the signals of the α-methylene group in the tetrabutylammonium cation (about 3.1 ppm). The ratios of N- to O-alkylation and azoxy to N-alkylated products were obtained by integration of the −COO**CH$_2$**CH$_3$ signals in the products as well as some characteristic peaks for the alkyl substituents. The results are listed in Table 2.

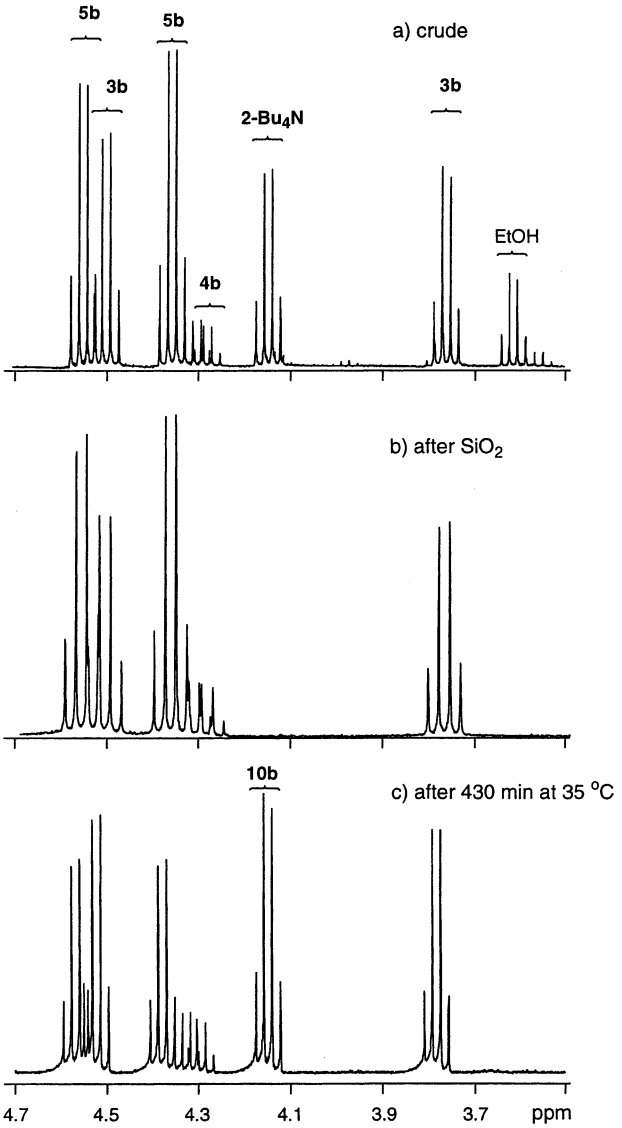

Figure 1. Low field portion of NMR spectra of the reaction mixture of **2-Bu$_4$N** with ethyl iodide in CD_2Cl_2: (a) spectrum of crude reaction mixture recorded after 105 min at 0 °C and then 20 min at 25 °C, (b) recorded after passing the crude reaction mixture through a SiO_2 plug, and (c) mixture shown in panel b after 430 min at 35 °C. Spectra recorded at 400 (panels a and c) and 300 MHz (panel b) instruments.

Alkylation reactions with methyl iodide and benzyl bromide were completed within 1 h at 0 °C, while those with ethyl and isopropyl iodides required ambient temperature to achieve appreciable reaction rates. At this temperature, however, thermal decomposition of **2-Bu$_4$N** competes with the alkylation reaction. The observed qualitative differences in reactivity of the alkyl electrophiles are in good agreement with the general reactivities of alkyl halides with nucleophiles.[37]

Stability of the Anion 2 and the *O*-Alkyl Derivatives 1. ^{1}H NMR studies of the pure salt showed that anion **2** was cleanly converted into two new products over several hours at ambient

(34) Moss, R. A. *Tetrahedron Lett.* **1966**, *7*, 711−718.
(35) Fugmann, B.; Steglich, W. *Angew. Chem., Int. Ed. Engl.* **1984**, *23*, 72−73.
(36) Broxton, T. J.; Stray, A. C. *Aust. J. Chem.* **1982**, *35*, 961−972.
(37) Streitwieser, A. J. *Solvolytic Displacement Reactions*; McGraw-Hill: New York, 1962; p 13.

Table 1. Characteristic ^{1}H NMR Chemical Shifts for Alkyl Halides and Observed Products in Alkylation of Ethyl *N*-Nitrosocarbamate Salt **2-Bu$_4$N**[a]

R	solvent	R-I	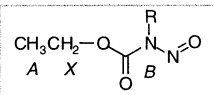 **3**			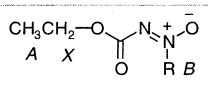 **4**			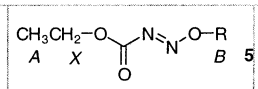 **5**			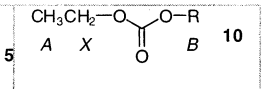 **10**		
			A	*X*	*B*	*A*	*X*	*B*	*A*	*X*	*B*	*A*	*X*	*B*
Me	CD_2Cl_2	2.15 (s, 3H)	1.37	4.50	3.12		4.29	4.12		4.35	4.11	experiment not run		
(**a**)	CD_3CN	2.15 (s, 3H)	1.36	4.46	3.07		4.27	4.13		4.35	4.10	experiment not run		
	$CDCl_3$		[b] 1.48	4.57	3.17									
Et	CD_2Cl_2	1.80 (t, 3H), 3.19 (q, 2H)	1.44	4.50	3.77 and 0.99	1.54	4.29	4.32 and 1.33	1.37	4.37	4.56 and 1.41	1.28	4.15	4.15 and 1.28
(**b**)	CD_3CN	1.77 (t, 3H), 3.22 (q, 2H)		4.51	3.78		4.32	4.34		4.39	4.58			
	$CDCl_3$		1.47	4.59	3.80 and 1.02							1.31	4.19	4.19 and 1.31
i-Pr	CD_2Cl_2	1.86 (d, 6H), 4.34 (sept, 1H)		4.30	4.56	not observed				4.35	4.98	experiment not run		
(**c**)	CD_3CN	1.83 (d, 6H), 4.38 (sept, 1H)		4.29	4.58	not observed				4.34	4.98	experiment not run		
	$CDCl_3$		[c] 1.38	4.37	4.59 and 1.56									
$PhCH_2$	CD_2Cl_2	[d] 4.51 (s, 2H)	1.43	4.54	4.91		4.27[f]	5.33[f]	1.38	4.39	5.52	1.29	4.19	5.14
(**d**)	CD_3CN	[d] 4.58 (s, 2H)	1.30	4.49	4.88		4.28[f]	5.39[f]	1.36	4.34	5.51			
	$CDCl_3$		[e] 1.46	4.56	4.93							[g] 1.32	4.22	5.17

[a] The signals for the products were assigned based on matching intensities for multiplets and general trends in ^{1}H NMR chemical shifts. The A_3X_2 signal of the ethyl group in the starting **2-Bu$_4$N**: (CD_2Cl_2) δ 1.27 (t, J = 7.1 Hz, 3H), 4.14 (q, J = 7.1 Hz, 2H); (CD_3CN) δ 1.23 (t, J = 7.1 Hz, 3H), 4.08 (q, J = 7.1 Hz, 2H). [b] Ref 15: ^{1}H NMR ($CDCl_3$) δ 1.46 (t, J = 7.1 Hz, 3H), 3.15 (s, 3H), 4.55 (q, J = 7.1 Hz, 2H). [c] Ref 34: ^{1}H NMR (CCl_4) δ 1.42 (t), 4.44 (q), 4.80 (m). [d] Benzyl bromide. Aromatic part not shown. [e] Ref 15: ^{1}H NMR ($CDCl_3$) δ 1.43 (t, J = 7.2 Hz, 3H), 4.54 (q, J = 7.2 Hz, 2H), 4.90 (s, 2H), 7.22 (s, 5H). Ref 34: ^{1}H NMR (CCl_4) δ 1.30 (t), 4.55 (q), 4.93 (s). [f] Assignment is uncertain. [g] Ref 66: ^{1}H NMR ($CDCl_3$) δ 1.25 (t, 3H), 4.15 (q, 2H), 5.1 (s, 2H), 7.35 (s, 5H).

Table 2. Ratio of Alkylation Products of Ethyl *N*-Nitrosocarbamate Anion[a]

		CD_2Cl_2			CD_3CN		
R	*T* (°C)	**5/3** ratio	**4/3** ratio	total yield (%)	**5/3** ratio	**4/3** ratio	total yield (%)
Me	0	0.2	0.05	95	0.2	0.03	95
Et	20	1.4	0.2	85	1.2	0.2	65
i-Pr	20	6.7	*b*	40	7.1	0.0	60
$PhCH_2$	0	1.0	0.08	95	0.9	0.03	95

[a] Established by integration of ^{1}H NMR signals. See text for details. [b] Solvent peak interference.

Scheme 5

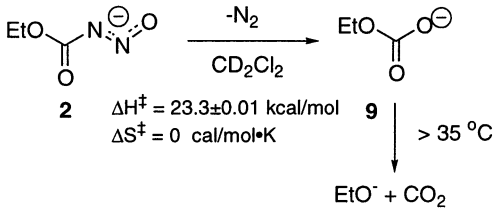

temperature in either CD_2Cl_2 or CD_3CN. The upfield A_3X_2 signal (1.06 and 3.51 ppm in CD_3CN) was identified as ethanol by comparison with an authentic sample. The downfield A_3X_2 signal (1.09 and 3.71 ppm) was assigned to the ethyl carbonate anion (**9**), which was converted to ethanol upon heating the reaction mixture to 80 °C for 1 h (Scheme 5). The observed chemical shifts for **9** are consistent with those reported for ethoxycarbonate salts of palladium and zinc complexes.[38,39]

Kinetic measurements show that the decomposition of **2-Bu$_4$N** in CD_2Cl_2 is a first-order process with an activation enthalpy $\Delta H^{\ddagger}$= 23.3 ± 0.01 kcal/mol and entropy $\Delta S^{\ddagger}$ = 0 cal/mol·K within experimental error (for details see the Supporting Information).

Scheme 6

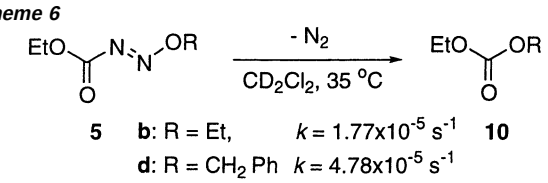

The thermal stability of O-isomers **5b** and **5d** was assessed using mixtures of alkylated regioisomers isolated from the reactions of **2-Bu$_4$N** in CH_2Cl_2 by flash chromatography. During the isolation process the ratio of O/N products decreased, indicating that about 15% of the O-isomer decomposed upon contact with silica gel and handling at ambient temperature. The salt-free solutions of the regioisomers in CD_2Cl_2 were monitored at 35 °C by ^{1}H NMR. As the reaction proceeded, the signals characteristic for O-isomers **5** disappeared simultaneously with the appearance of only one new set of signals assigned to alkyl ethyl carbonate **10** (Figure 1 and Scheme 6).

Monitoring of the ratio of the *O*-alkyl derivative to the *N*-alkyl regioisomer showed that the decomposition of **5** in CD_2Cl_2 is a first-order process with rate constants $k = 1.77 \pm 0.02 \times 10^{-5}$ s^{-1} for **5b** and $k = 4.78 \pm 0.08 \times 10^{-5}$ s^{-1} for **5d**. This compares to $k = 18.5 \pm 0.1 \times 10^{-5}$ s^{-1} for the decomposition of anion **2-Bu$_4$N** under identical conditions. The same measurements performed for **5d** in CD_3CN gave $k = 3.20 \pm 0.01 \times 10^{-5}$ s^{-1}. The formation of carbonate **10** is concomitant with the disappearance of the *O*-alkyl derivative **5**, and the process is also first-order. The absolute values of the rate constants for the two processes measured for **5d** in CD_2Cl_2 are approximately equal.

Quantum-Mechanical Calculations. To provide a better understanding of the chemical processes and transformations involving **2**−**5**, a series of calculations at the MP2(fc)/6-31+G-(d)//MP2(fc)/6-31G(d) level were performed. Thus, conforma-

(38) Ozawa, F.; Son, T.; Ebina, S.; Osakada, K.; Yamamoto, A. *Organometallics* **1992**, *11*, 171−176.

(39) Kato, M.; Ito, T. *Inorg. Chem.* **1985**, *24*, 504−508.

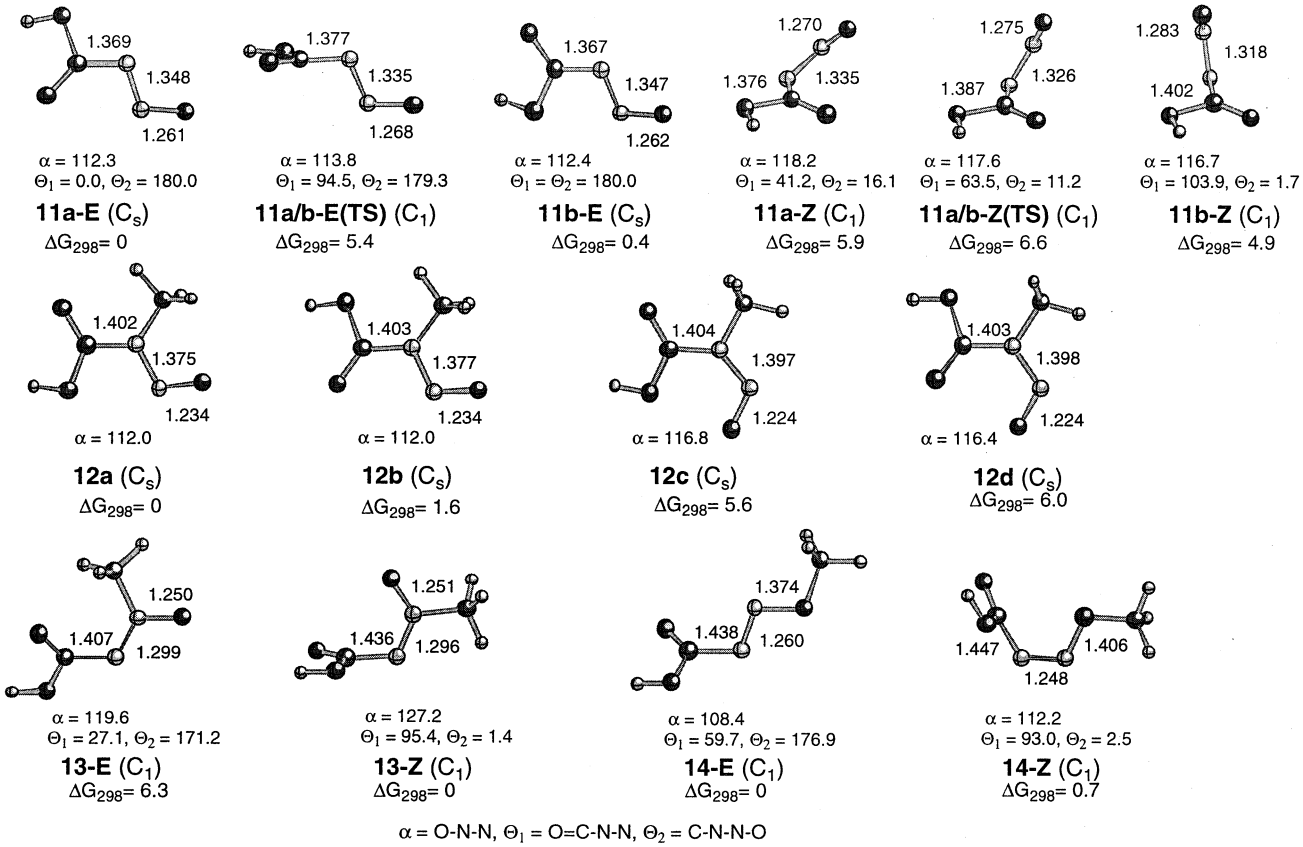

Figure 2. Optimized (MP2(fc)/6-31G(d)) geometries of ground and transition state structures for selected compounds. Relative energies in kcal/mol were computed at the MP2(fc)/6-31+G(d)//MP2(fc)/6-31G(d) level of theory.

tional analysis for *N*-carboxydiazotate anion (**11**) and three methylation products **12**−**14** established the structures and energies for their global conformational minima. Transition structures for cis−trans isomerization of **11**−**14** were calculated. Subsequently, the transition structures, and the pre- and post-transition complexes for gas-phase alkylation reactions of **11** with CH_3Cl were located. Finally, unimolecular thermal decomposition reactions of anion **11** and the methyl derivatives **12**−**14** were investigated.

Conformational Analysis and Ground State Structures. Calculations show that the planar (C_s) *trans*-diazotate anion **11a-E** (Figure 2) with the s-cis configuration of the C−N bond represents the global minimum on the potential energy surface (PES). The planar s-trans conformer **11b-E** represents a local minimum on the PES and is less thermodynamically stable than the planar s-cis isomer **11a-E** by $\Delta G_{298} = 0.4$ kcal/mol (Figure 2). The two conformers interconvert through a transition structure **11a/b-E(TS)** and a barrier $\Delta G^{\ddagger}_{298} = 5.4$ kcal/mol.

Two conformers of the *cis*-diazotate anion, **11a-Z** and **11b-Z**, are nonplanar in their equilibrium geometries and are thermodynamically less stable than **11a-E** by $\Delta G_{298} = 5.9$ and 4.9 kcal/mol, respectively (Figure 2). While the O=C−N−N dihedral angle in the pseudo-s-cis conformer **11a-Z** is $\theta = 41.2°$, the analogous pseudo-s-trans structure could not be located on the PES. Instead, structure **11b-Z** with a pseudo-orthogonal orientation of the COOH group with respect to the N−N−O plane ($\theta = 103.9°$) was found. The syn orientation of the two groups in **11b-Z** results in close contact between the carbonyl group and the oxygen atom ($d_{C\cdots O} = 2.461$ Å), which presumably provides additional stabilization. Conformer **11b-Z** converts to **11a-Z** through transition state **11a/b-Z(TS)** with a barrier $\Delta G^{\ddagger}_{298} = 1.7$ kcal/mol.

Conformational analysis of the N-methylation product found four planar ground state structures, among which **12a** represents the global minimum on the PES. The calculated 1,2-anti-2,3-anti configuration of **12a** is consistent with the results of previous calculations for the methyl ester of **12**[40] and the reported solid state structure of *N*,*N*′-dimethylnitrosourea.[41] The rotation of the carboxyl group around the C−N bond leads to **12b** with a 1,2-syn-2,3-anti configuration, which is less thermodynamically stable than **12a** by $\Delta G_{298} = 1.6$ kcal/mol. A much larger decrease in thermodynamic stability is observed for conformers with a syn orientation between the carboxyl and the nitroso groups. For instance, **12c** with a 1,2-anti-2,3-syn configuration is less stable than **12a** by $\Delta G_{298} = 5.6$ kcal/mol. This is consistent with literature results for the methyl ester of **12**.[40] A nonplanar structure with the s-cis configuration of the N−N bond could not be located on the PES, and the resulting equilibrium molecular geometry was that of **12c**. The interconversion of the methyl ester of **12a** to its methyl analogue of **12c** requires $\Delta E_0 = 17.4$ kcal/mol of activation energy.[40] Optimized geometries for conformers **12a**−**d** are shown in Figure 2, and the structures and data for all conformers are listed in the Supporting Information.

A conformational search for azoxy derivative **13** located only one trans isomer **13-E** and one cis isomer **13-Z** on the PES (Figure 2). The latter was found to be more thermodynamically stable than the trans isomer by $\Delta G_{298} = 6.3$ kcal/mol. The trans isomer **13-E** adopts a s-cis configuration around the C−N bond. In contrast, the carboxyl group in the cis isomer **13-Z** is almost

(40) Nakayama, N.; Kikuchi, O. *J. Mol. Struct. (THEOCHEM)* **2001**, *536*, 213−218.
(41) Prout, K.; Fail, J.; Hernandez-Cassou, S.; Miao, F. M. *Acta Crystallogr.* **1982**, *B38*, 2176−2181.

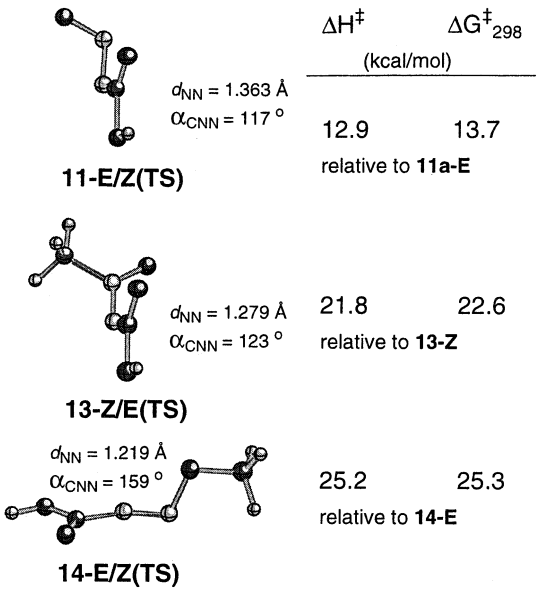

Figure 3. Optimized (MP2(fc)/6-31G(d)) geometries of transition state structures for cis−trans isomerization. Relative energies in kcal/mol were computed at the MP2(fc)/6-31+G(d)//MP2(fc)/6-31G(d) level of theory. Bond orders are given in Table 3.

orthogonal to the N═N−O group ($\theta_{O=C-N-N} = 95.4°$), which results in a short carbonyl−oxygen nonbonding distance ($d_{C\cdots O} = 2.571$ Å).

Similar results were obtained for diazene **14**, and only one conformer for the cis and one for the trans isomers were found on the PES (Figure 2). The carboxyl group in **14-E** adopts a pseudo-s-cis configuration with respect to the diazene, while in the cis isomer **14-Z** the groups are practically orthogonal ($\theta_{O=C-N-N} = 93.0°$). Both isomers are nearly isoenergetic with a slight preference for the trans methoxydiazene **14-E** ($\Delta G_{298} = 0.7$ kcal/mol).

A comparison of the computational results for all three regioisomers indicates that the azoxy and *O*-methyl derivatives, **13-Z** and **14-E**, are less stable by about 7 and 13 kcal/mol, respectively, than the *N*-methyl isomer **12a**.

Cis−Trans Isomerization. The STQN calculations located the transition structures **11-E/Z(TS)**, **13-Z/E(TS)**, and **14-E/Z(TS)** for isomerization about the N═N double bond in the anion **11**, azoxy **13**, and diazene **14**, respectively (Figure 3). The activation energies listed in Figure 3 show that anion **11** has the lowest cis−trans interconversion barrier, and the highest is calculated for the diazene **14**.

Inspection of the nuclear motions associated with the negative frequency in the normal modes shows that the isomerization in anion **11a** and azoxy **13** occurs by rotation around the N═N bond, while in diazene **14** it occurs by inversion at the N(2) atom. These mechanistic pathways are consistent with changes of bond order and charge distribution between the ground and the transition states. Thus, for anion **11** and azoxy **13** the N−N Wiberg bond order index (WBOI) decreases in the transition state, while for diazene **14** the bond order slightly increases (Table 3). The calculated activation energies and the observed trend are consistent with those reported in the literature for other compounds containing the azo group.[42]

Methylation of Anion 11. The WBOI for **11a-E** shows that the O−N−N−C−O atoms are conjugated, with a significant development of double bond character for the N−N and N−C bonds at the expense of the N═O and C═O bonds (Figure 4). Consequently, the negative charge is delocalized over the five atom array and, in analogy to the pentadienyl anion, concentrated in positions 1, 3, and 5. Analysis of the electronic structure shows that the HOMO for **11a-E** is a combination of three lone pairs at two nitrogen atoms and one oxygen atom, while the HOMO-1 is the highest orbital corresponding to the π electron manifold. The graphical representation for the two almost isoenergetic MOs is shown in Figure 5. A very similar charge and MO distribution was found for the s-trans conformer, **11b-E**.

According to calculations, the two trans conformers, **11a-E** and **11b-E**, are in equilibrium in solution in a ratio of about 2:1, and both can undergo alkylation reactions. In contrast, the concentration of the cis isomer **11-Z** is expected to be 4 orders of magnitude lower than the trans isomer and not compete for the electrophile.

Investigations of gas-phase alkylation reactions of anion **11-E** with methyl chloride located transition structures **11TS12**, **11TS13**, and **11TS14** as well as the corresponding pre- and post-transition complexes for the formation of three regioisomers **12**−**14**, respectively (Figure 6). In the formation of azoxy **13**, the Cl(−) anion deprotonates the carboxyl group and the post-transition complex is not shown.

Table 3. WBOI for Selected Compounds

compound	WBOI O═C	C–N	N═N	N–O
11a-E	1.54	1.24	1.33	1.63
11-E/Z(TS)	1.44	1.41	1.16	1.79
13-Z	1.64	1.06	1.47	1.51
13-Z/E(TS)	1.58	1.15	1.34	1.65
14-E	1.73	0.97	1.90	1.05
14-E/Z(TS)	1.63	1.10	1.96	0.98

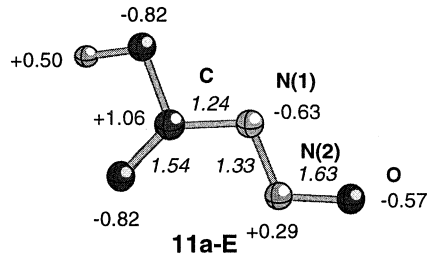

Figure 4. Calculated (MP2(fc)/6-31+G(d)//MP2(fc)/6-31G(d)) natural charge density and WBOI (italics) in the diazotate ion **11a-E**.

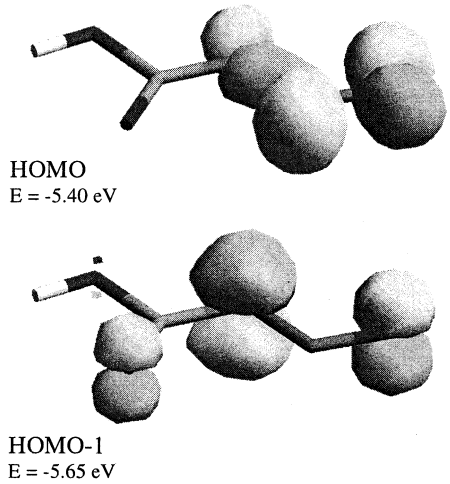

Figure 5. Representation of the HOMO and HOMO-1 calculated (MP2(fc)/6-31+G(d)//MP2(fc)/6-31G(d)) for the diazotate ion **11a-E**.

(42) Kalinowski, H.-O.; Kessler, H. *Top. Stereochem.* **1973**, *7*, 295−383.

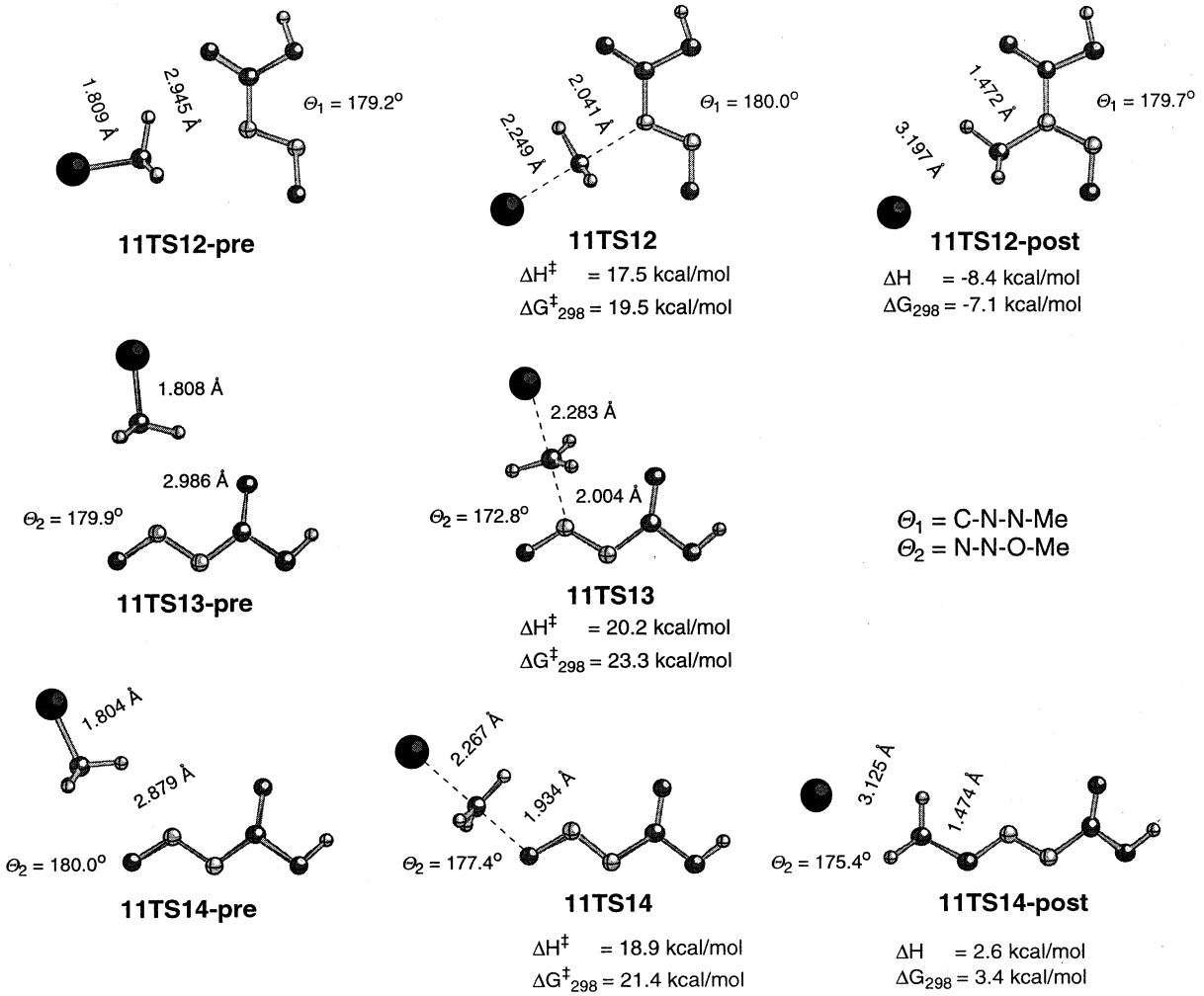

Figure 6. Optimized (MP2(fc)/6-31G(d)) geometries of transition states and pre- and post-transition complexes for alkylation of anion **11** with MeCl. Relative energies in kcal/mol were computed at the MP2(fc)/6-31+G(d)//MP2(fc)/6-31G(d) level of theory.

In all three reactions the electrophile approaches the nucleophile in the π plane, and consequently all complexes and transition structures are planar or close to planarity, as indicated by θ_1 and θ_2 in Figure 6. This suggests that the electrophile interacts with the anion lone pairs that constitute the anion's HOMO (Figure 5). The lowest activation energy of $\Delta G^{\ddagger}_{298} =$ 19.5 kcal/mol was calculated for the N-alkylation and the highest activation energy was found for the formation of the azoxy derivative **13** ($\Delta G^{\ddagger}_{298} =$ 23.3 kcal/mol).

The formation of **13** and **14** begins with the s-cis conformer **11a-E**. In contrast, the formation of **12** proceeds through transition structure **11TS12** derived from the less thermodynamically stable s-trans form of the anion, **11b-E**. The product derived from **11a-E** would lead to a conformational transition structure, while methylation of **11b-E** gives **12a**, which represents the global conformational minimum for **12**. This preference for the orientation of the COOH group is presumably dictated by the generally more favorable steric interaction between the methyl group and the carbonyl, C−H···O=C, rather than analogous interactions with the OH group, C−H···O−C in the transition state.

The N(1) and O-alkylation reactions lead directly to the most thermodynamically stable isomers **12a** and **14-E**, respectively. In contrast, N(2) methylation results in the less thermodynamically stable trans isomer **13-E**, which is likely to convert to the thermodynamic product **13-Z** through a relatively low isomerization barrier of $\Delta G^{\ddagger}_{298} =$ 16.3 kcal/mol. Results for all three

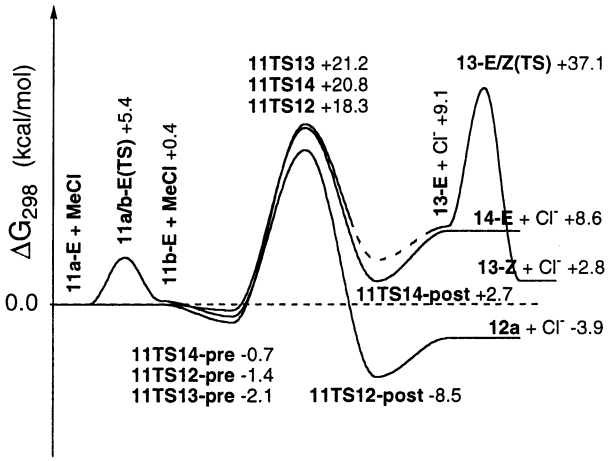

Figure 7. MP2(fc)/6-31+G(d)//MP2(fc)/6-31G(d) Gibbs free-energy profiles (298 K) for the alkylation reactions of anion **11** in the gas phase. Ground and transition state structures are shown in Figures 2 and 6.

alkylation processes are presented graphically in Figure 7 , and full computational data is listed in the Supporting Information.

Decomposition Processes. The experimental data suggest that the decomposition of anion **2** and alkoxydiazene **5** and the formation of carbonates **9** and **10**, respectively, are concerted and related processes. Both processes require direct interactions of the oxygen atom bound to the nitrogen atom with the carbonyl

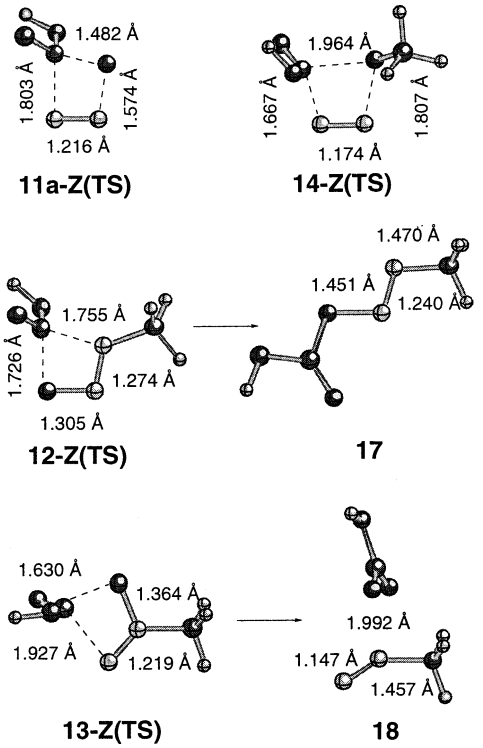

Figure 8. Optimized (MP2(fc)/6-31G(d)) geometries of transition states for concerted decomposition of anion **11** and its alkylation products. Relative energies in kcal/mol were computed at the MP2(fc)/6-31+G(d)//MP2(fc)/6-31G(d) level of theory. The C−N−N−O angle in all transition structures is less than 2°.

Table 4. Activation Energies for Decomposition and Rearangement Reactions

compound		$\Delta H^{\ddagger}$ (kcal/mol)	$\Delta S^{\ddagger}$ (cal/mol·K)
11	(calcd)[a]	15.2	−2.5
2-Bu$_4$N	(exptl)	23.3	0.0
12	(calcd)[a]	29.3	−1.4
3a	(exptl)[b]	29.4	−3.8
13	(calcd)[a]	39.6	−3.8
14	(calcd)[a]	25.2	−0.4

[a] MP2(fc)/6-31+G(d)//MP2(fc)/6-31G(d) calculations. [b] Ref 43.

group carbon atom in a four-center transition state. A similar process has been proposed as a first step in the decomposition of **3**[1,43] and can also be envisioned for the intramolecular rearrangement of the azoxy derivatives **4**.

A transition state search located structures **11-Z(TS)** and **14-Z(TS)**, which are higher in energy than the corresponding local minima (**11b-Z** and **14-Z**) by $\Delta G^{\ddagger}_{298}$ = 15.9 and 20.7 kcal/mol, respectively (Figure 8). The gas-phase calculated activation energy for the decomposition of **11** is significantly lower than the experimental value of $\Delta G^{\ddagger}_{298}$ = 23.3 kcal/mol measured for **2-Bu$_4$N** in solution (Table 4). Analysis of molecular structures confirmed the four-center cyclic transition states **11-Z(TS)** and **14-Z(TS)** in which the O···CO distance is 1.482 and 1.964 Å, respectively.

The cis isomers required for the concerted decomposition reaction are accessible from the more thermodynamically stable trans isomers through a trans−cis isomerization process. Both overall decomposition processes are highly exothermic by about 90 kcal/mol with respect to precursors **11a-E** and **14-E**. A

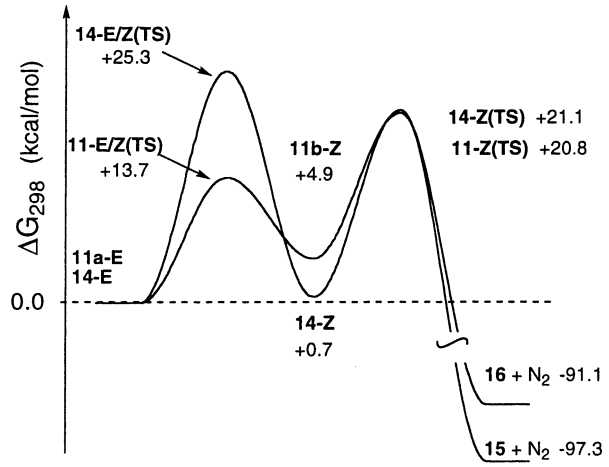

Figure 9. MP2(fc)/6-31+G(d)//MP2(fc)/6-31G(d) Gibbs free-energy profiles (298 K) for the concerted decomposition of anion **11** and diazene **14** in the gas phase. Ground and transition state structures are shown in Figures 2 and 8.

Scheme 7

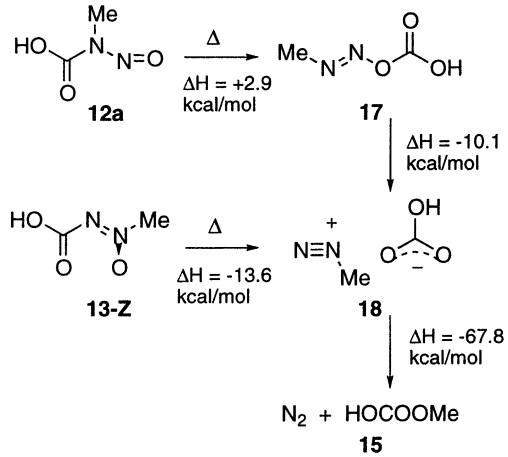

graphical representation of the entire decomposition process is shown in Figure 9.

An alternative nonconcerted decomposition of **14-E** through the homolysis of the O−N bond and formation of a radical pair is calculated to be significantly endothermic (ΔH = 50.5 or ΔG_{298} = 37.7 kcal/mol) and almost certainly does not compete with the concerted mechanism under the reaction conditions. The overall ΔG_{298} for breaking the two bonds is only slightly negative by −6.0 kcal/mol. The feasibility of the nonconcerted heterolytic process is difficult to assess without an adequate solvation model, and it was not attempted here.

Elimination of N_2 from **3** and **4** in a concerted process is not possible because of the presence of an alkyl substituent on the nitrogen atoms. Therefore, their decomposition is necessarily a two-step process involving an intramolecular rearrangement through a four-center transition state, followed by a heterolytic cleavage of the N−O bond in the resulting intermediate ester as shown in Scheme 7 for the model analogues **12** and **13**.

Indeed, calculations located four-centered transition states **12-Z(TS)** and **13-Z(TS)** that lead to azo ester **17** and ion pair **18** (Figure 8). The calculated activation energies for the rearrangement are significantly higher than those found for **11** and **14** and are $\Delta G^{\ddagger}_{298}$ = 29.7 and 40.7 kcal/mol for **12-Z** and **13-Z**, respectively (Table 4). The activation energy for **12-Z** compares very well to the experimental value of $\Delta G^{\ddagger}_{298}$ = 30.5 ± 1.2 kcal/mol measured for **3a** in pseudocumene.[43] Ester **17** is less

(43) Huisgen, R.; Reimlinger, H. *Justus Liebigs Ann. Chem.* **1956**, *599*, 161−182 and 183−202.

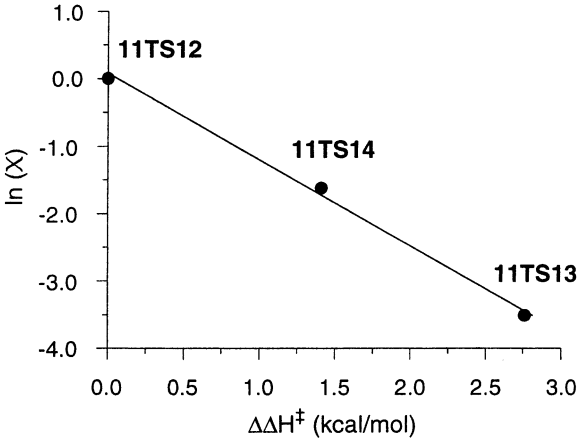

Figure 10. Correlation between experimental relative yields of products for methylation of **2-Bu$_4$N** and calculated (MP2(fc)/6-31+G(d)//MP2(fc)/6-31G(d)) enthalpy of activation $\Delta H^{\ddagger}$ for methylation of **11a-E**. *X* represents a ratio of three regioisomers **3a**, **4a**, and **5a** to **3a** (Table 2).

thermodynamically stable than the starting compound **12a** by $\Delta G_{298} = 2.9$ kcal/mol, but upon ionization it converts to ion pair **18** with an exotherm $\Delta G_{298} = -10.2$ kcal/mol. This is consistent with the accepted mechanism for the degradation of **3**.[44,45] The subsequent reaction of methanediazonium cation with a nucleophile, such as the carbonate anion, brings the overall exothermicity of the decomposition of **12** and **13** to over 70 kcal/mol in the gas phase.

Discussion

Experimental results show that the methylation of the ambident ethoxycarbonyldiazotate anion **2** occurs preferentially at the N(1) site leading to nitrosourethane **3a**, while the other two isomers **4a** and **5a** are formed in significantly smaller quantities. The observed distribution of products is practically solvent-independent and correlates well with the theoretical activation energies E_a. Figure 10 shows a plot of the difference in enthalpy of activation versus the ln of the ratio of isomers both relative to **3a** (Table 2). The best fit line has a slope of 1.27, which is smaller than the ideal value of 1.84 for a reaction carried out at 0 °C. This suggests that the actual activation energies for the reaction of **2** with MeI in solution are smaller by a factor of 1.45 than those calculated for **11** and MeCl in the gas phase. Besides the systematic computational error, the difference in activation energies presumably reflects two competing effects related to the reaction medium and the nature of the electrophile. Typically, a change of reaction medium from gas phase to dipolar aprotic solvent increases E_a,[46,47] while substituting MeI for MeCl decreases E_a.[48] Both effects are of similar magnitudes and, based on the available data,[46,47,49,50] the electrophile effect is dominant. This is consistent with the value of the slope in Figure 10.

Increasing steric demand of the electrophile results in an increase of the diazene/nitroso (**5**/**3**) ratio from about 0.2 for methyl to about 7 for isopropyl. Again, the ratio of products is virtually solvent-independent, suggesting that the anion is practically free in both solvents. Unfortunately, the increase of relative yield of **5** is concomitant with a decrease of the overall yield of the reaction because of the competitive thermal decomposition of anion **2**. The azoxy/nitroso ratio (**4**/**3**) also increases for ethyl, but in the reaction with isopropyl iodide **4c** was not detected. Similar results were observed for alkylation of arenediazotate anions in DMSO or DMF, but no azoxy compound has been isolated or reported.[17]

The observed regioselectivity in alkylation of **2** and arene analogues is in sharp contrast with the results of alkylation of alkanediazotates in HMPTA, which show azoxy and *O*-alkyl derivatives as the major products.[14] This difference in distribution of the regioisomers is most likely related to the distribution of electron density in the ambident anions. Since the alkyl group does not stabilize the negative charge on N(1), the electron density is shifted from N(1) toward the oxygen atom enhancing nucleophilicity of N(2) and O in alkanediazotates in comparison with nitrosourethane anion **2**. Thus, the positive charge on the N(2) atom decreases from +0.26 in **2** to +0.18 in MeN=NO-(−), and the negative charge on the oxygen increases by 0.18, according to NBO calculations. Steric shielding of the N(1) nitrogen atom by the alkyl group is likely to be another factor affecting the regioselectivity of the alkylation.

Theoretical analysis of the alkylation reaction of **2** reveals that the electrophile approaches the anion in the π plane. This closely resembles the computational results for alkylation of enolates in which the in-plane attack on the oxygen lone pair has a substantially lower activation energy when compared to C-attack, which is necessarily perpendicular to the π plane.[29−31] The O-attack is less sterically demanding and does not require disruption of conjugation in the transition state. Unlike enolates, all three atoms (two N and one O) in diazotates have unshared electron pairs (Figure 5) that can participate in transition states without involving the π electrons.

According to the results of NBO calculations for **11a-E**, the Mulliken charges on the oxygen and nitrogen N(1) atoms are similar and significantly negative, while the central nitrogen atom N(2) has a net positive charge (Figure 4). Since under similar circumstances nitrogen is known to be more nucleophilic than oxygen and the electron density of the two atoms in the diazotate anion is comparable, the N(1) center would effectively compete for the electrophile, as long as it is not too sterically shielded. In contrast, the second nitrogen atom N(2) is expected to be much less competitive for the electrophile largely because of low electron density. These qualitative arguments are in good agreement with the observed distribution of products and results of theoretical analysis for **2** and also for alkanediazotates (vide supra).

Calculations demonstrate that the concerted four-center mechanism for the decomposition of anion **2** and azene **5** is consistent with reaction products (carbonates **9** and **10**, respectively) and that the transition states are energetically accessible under the experimental conditions. The mechanistically required cis isomers **2-Z** and **5-Z** are presumably formed in situ by isomerization of the corresponding trans isomers.

The anion **2-E** is in equilibrium with the less thermodynamically stable cis isomer **2-Z** through a relatively low interconversion barrier (calcd $\Delta G^{\ddagger}_{298} = 13.7$ kcal/mol; Figures 3 and 9). The cis isomer is present in small quantities and decomposes through a barrier of about $\Delta G^{\ddagger}_{298} = 23.3$ kcal/mol (calcd $\Delta G^{\ddagger}_{298} = 15.9$ kcal/mol), which represents the rate-determining step.

(44) White, E. H.; Field, K. W.; Henderickson, W. H.; Dzadzic, P.; Roswell, D. F.; Paik, S.; Mullen, P. W. *J. Am. Chem. Soc.* **1992**, *114*, 8023−8031.
(45) Darbeau, R. W.; Pease, R. S.; Gibble, R. E. *J. Org. Chem.* **2001**, *66*, 5027−5032.
(46) Tanaka, K.; Mackay, G. I.; Payzant, J. D.; Bohme, D. K. *Can. J. Chem.* **1976**, *54*, 1643−1659.
(47) Reichardt, C. *Solvents and Solvent Effects in Organic Chemistry*, 2nd ed; VCH: New York, 1990.
(48) Parker, A. J. *Chem. Rev.* **1969**, *69*, 1−32.
(49) Shaik, S. S.; Schlegel, H. B.; Wolfe, S. *Theoretical Aspects of Physical Organic Chemistry. The SN2 Mechanism*; Wiley and Sons: New York, 1992.
(50) Riveros, J. M.; José, S. M.; Takashima, K. In *Advances in Physical Organic Chemistry*; Gold, V., Bethell, D., Eds.; Academic Press: New York, 1985; Vol. 21, pp 197−240.

The 7.4 kcal/mol difference between the theoretical and experimental activation energies can be ascribed to solvent interactions with the anion.[47] Similar solvation effects can be expected for the trans−cis isomerization of **2**. Consequently, the relative difference between activation energy for isomerization and decomposition is expected to remain approximately the same in the gas phase and in solution.

In contrast to the reaction pathway for anion **2**, the trans−cis isomerization of diazene **5** is the rate-determining step and requires higher energy (calcd $\Delta G^{\ddagger}_{298} = 25.3$ kcal/mol) than that for the decomposition through a four-center transition state (calcd $\Delta G^{\ddagger}_{298} = 21.1$ kcal/mol). Since **5** is a neutral molecule, solvent effects are expected to have relatively small impact on the energy. This is evident from the close match between experimental and theoretical $\Delta G^{\ddagger}_{298}$ values for the decomposition of another neutral compound, **3a** (Table 4).

The mechanistic analysis and computational results for **11** and **14** are consistent with experimental data for **2** and **5**. The observed nearly 10-fold higher rate for the decomposition of anion **2** than of azene **5** is consistent with the calculated lower stability of the former. Moreover, in both cases the cis isomers, **2-Z** and **5-Z**, are predicted to be transient species present in concentrations below the detection limit. This is in agreement with the fact that only single isomers for **2** and **5**, most likely **2-E** and **5-E**, are observed in the solution by NMR.

Rearrangement of nitrosourethane **3** and azoxy **4** through a similar concerted four-center mechanism requires significantly higher activation energies than those predicted for **2** and **5**. The value of $\Delta G^{\ddagger}_{298} = 29.7$ kcal/mol calculated for **12** is within the error bar of the experimental value of $\Delta G^{\ddagger}_{298} = 30.5 \pm 1.2$ kcal/mol obtained for **3a**,[43] which further validates the computational results. Considering the experimentally measured rate constant of $k = 0.016 \times 10^{-5}$ s^{-1} for **3a** at 70 °C,[43] compounds **3** and **4** should be thermally stable under our experimental conditions including heating for 1 h at 80 °C in MeCN. Surprisingly, azoxy **4**, with the highest calculated activation energy of $\Delta G^{\ddagger}_{298} = 40.7$ kcal/mol, disappeared from the NMR spectrum under these conditions. Since an authentic sample of **4b** shows no trace of decomposition in CD_3CN at 80 °C for 1 h, the observation made for the crude reaction mixture can be explained by the presence of a base generated from the decomposition of the anion **2**. Unlike the case of **2** and **5**, the products of the decomposition of **3** and **4** are unstable and undergo further heterolysis producing alkyldiazonium ions.

The cis−trans isomerization of the N═N bond plays an important role in the stability of the anion and the alkylation products. Generally, low isomerization barriers are expected for the allyl-type system, Y−N═N−Ẍ ↔ Y−N̈⁻−N═X⁺, in which X and Y reduce the bond order between the nitrogen atoms by sharing the lone pair of Ẍ and stabilizing the negative charge on the other nitrogen atom by Y. A very favorable combination of X and Y is found in nitrosourethane anion **2** in which the carboxyl group stabilizes the negative charge on the nitrogen atom. As a result, the isomerization requires low activation energy, typical for neutral nitrosoamines,[51] and proceeds through a rotation around the essentially single N−N bond (see **11-E/Z(TS)** in Figure 3 and Table 3). The energy for isomerization increases when the carboxyl group is replaced with an aromatic group[16,22,52,53] and is completely inhibited in alkanediazotates

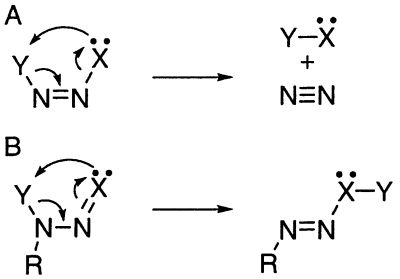

Figure 11. Generalized mechanisms for decomposition of nitroso and diazo derivatives.

at ambient temperature.[54] For instance, the measured cis−trans isomerization of 4-nitrobenzenediazotate is $\Delta G^{\ddagger}_{298} = 19.9$ kcal/mol,[53] while for the 4-(SO_3^-) analogue the barrier increases to $\Delta G^{\ddagger}_{298} = 24.7$ kcal/mol.[52] In methanediazotate, MeNNO(−), the barrier to cis−trans isomerization by rotation around the N−N bond is even higher, and $\Delta G^{\ddagger}_{298} = 43.8$ kcal/mol according to our calculations.[55] This is consistent with the ability to stabilize the negative charge on the N(1) atom.

A similar argument can be put forth for a relatively low energy for isomerization of the azoxy derivative **4** by rotation around the N−N bond. In contrast, isomerization of alkoxydiazene **5** appears to proceed through an inversion at the sp^2-hybridized nitrogen atom rather than the rotation around the N−N bond (see **14-E/Z(TS)** in Figure 3). This presumably results from the low ability of oxygen to share its lone pair with the N═N group to form a zwitterion with a low bond order between the nitrogen atoms.

In a broader perspective, the presented mechanism for the decomposition of **5** and **2** appears to be unique but also complementary to the well-accepted mechanism for the decomposition of **3** and related compounds[1,43−45,56] (Figure 11). In both mechanisms an electron lone pair on X attacks the electrophilic substituent Y leading to a four-center transition state, which requires the cis configuration of the N−N bond. It should be emphasized, however, that these rearrangements proceed through four-center transition states and *not* through four-membered heterocyclic intermediates, as is suggested in some recent literature. The substrates in transformations through mechanisms A and B in Figure 11 differ in the position of the double bond, which defines the reaction outcome. In mechanism A, the N═N double bond in the substrate leads to the formation of N_2 (decomposition of **2** and **5**) or diazonium ion (decomposition of **4**), while in mechanism B the substrate with an N−N bond rearranges to a product with an N═N bond (e.g., rearangement of **3**).

The nucleophilic substituent X typically is an oxygen atom associated with the nitroso, nitro, or alkoxy group. A nitrogen atom could also serve as the required internal nucleophile, and *i*-PrOOC−N═N−NMe_2 [57] could, in principle, rearrange via mechanism A. The triazene can be distilled at 65 °C, and its thermal stability is presumably due to steric demand of the alkyl substituents in the concerted TS.

The electrophilic Y typically is a carbonyl group in an amide, carbamate, or urea, but a sulfonyl group has also been suggested.[1,58] It is possible that the high propensity of *cis*-4-

(51) For example: (a) Olszewska, T.; Milewska, M. J.; Gdaniec, M.; Maluszynska, H.; Polonski, T. *J. Org. Chem.* **2001**, *66*, 501−506. (b) Miura, M.; Sakamoto, S.; Yamaguchi, K.; Ohwada, T. *Tetrahedron Lett.* **2000**, *41*, 3637−3641.
(52) Le Fèvre, R. J. W.; Sousa, J. B. *J. Chem. Soc.* **1955**, 3154−3159.
(53) Ketlinskii, V. A.; Bagal, I. L. *J. Org. Chem. USSR* **1973**, *9*, 1932−1935.
(54) Lown, J. W.; Chauhan, S. M. S.; Koganty, R. R.; Sapse, A.-M. *J. Am. Chem. Soc.* **1984**, *106*, 6401−6408.
(55) Our results are consistent with the 48.8 kcal/mol barrier to *Z*−*E* isomerization in the neutral methanediazohydroxide calculated as ΔSCF at the HF/6-31G* level of theory in ref 54.
(56) White, E. H.; Woodcock, D. J. In *The Chemistry of the Amino Group*; Patai, S., Ed.; Interscience: New York, 1968; pp 407−497.
(57) Egger, N.; Hoesch, L.; Dreiding, A. S. *Helv. Chim. Acta* **1983**, *66*, 1416−1426.

$NO_2C_6H_4$—N═N—OMe[59] toward elimination of N_2 and the formation of Ar—OMe at low temperature can be explained by the participation of the ipso carbon atom in the transition state according to mechanism A in Figure 11.

The mechanism shown in Figure 11 represents a concerted alternative to a nonconcerted heterolytic or homolytic decomposition pathway for the considered compounds. It can be speculated that the choice between these mechanisms depends largely on (i) the ability of the molecule to adopt the cis configuration (relative thermodynamic stability of the conformers and cis—trans isomers[43,60]), (ii) the ability of groups Y and R to support the positive charge, and (iii) the medium (polarity, protic solvents, and pH[61]). For simple systems such as compounds **2**—**5** in nonpolar and nonprotic solvents the concerted pathway appears to be preferred.

Finally, the experimental and computational data allow us to comment on a report describing the isolation of methoxydiazene **5a** from a reaction of **2-Ag** and MeI and its purification by vacuum distillation at 84 °C.[9] The preparation could not be repeated in our lab, and the thermal stability of **5a** required for distillation is doubtful. On the basis of the decomposition rate constant measured for **5b** ($k = 1.77 \times 10^{-5}$ s^{-1}) at 35 °C and the calculated activation energy for **14-Z** (25.3 kcal/mol), the estimated half-lifetime for **5a** at 84 °C is about 2 min.

Conclusions

Alkylation of an essentially free diazotate anion **2** in solution gives three regioisomers in yields that are affected by the nature of the electrophile. With more bulky electrophiles, the less thermodynamically stable diazene **5** dominates among the products, but its yield is compromised by the competing decomposition of the diazotate anion **2**. The observed low yield of **5** in the reactions of **2-Bu$_4$N** can perhaps be increased to a practical level by using stronger electrophiles and larger ester groups. Diazene **5** shows moderate stability at ambient temperature and low sensitivity to silica gel, which offers a method for isolating the pure material for further studies.

The MP2 level calculations are in agreement with experimental observations. They reveal the mechanistic complexity and suggest a four-center transition state for the decomposition of the nitrosourethane anion and its three alkylation regioisomers: *N*-nitroso, azoxy, and diazotate compounds. It is expected that the postulated mechanism is general for relative compounds in aprotic solvents.

Computational Details. Quantum-mechanical calculations were carried out initially at the B3LYP/6-31G(d) and finally at the MP2(fc)/6-31G(d) level of theory using the Linda—Gaussian 98 package[62] on a Beowulf cluster of 16 processors. Geometry optimizations were undertaken using appropriate symmetry constraints and default convergence limits. Global conformational minima were located at the B3LYP/6-31G(d) level of theory by setting different geometry constraints or by perturbing the geometry of the C_1-symmetry structures. Transition structures were obtained using the QST2 keyword at the B3LYP/6-31G(d) level of theory, which served as starting points for calculations at the MP2(fc)/6-31G(d) level of theory (keywords: TS, ReadFC). Vibrational frequencies were used to characterize the nature of the stationary points and to obtain thermodynamic parameters. Zero-point energy (ZPE) corrections for the MP2 results were scaled by 0.9670.[63] The WBOI were obtained using the NBO[64] algorithm supplied in the Gaussian package.

Following general recommendations,[65] energy changes and differences were derived as the differences of SCF energies of individual species computed using the diffuse function-augmented 6-31+G(d) basis set at the geometries obtained with the 6-31G(d) basis set (single-point calculations). Thermodynamic corrections were obtained using the 6-31G(d) basis set. All computational results discussed in the text were obtained at the MP2(fc)/6-31+G(d)//MP2(fc)/6-31G(d) level of theory, and the details are listed in Table S2 in the Supporting Information.

Experimental Section

^{1}H and ^{13}C NMR spectra were recorded at 400 and 100 MHz, respectively, and referenced to the solvent: CD_2Cl_2 δ 5.32 ppm for ^{1}H and 54.0 ppm for ^{13}C; CD_3CN δ 1.93 ppm; DMSO δ 2.49 ppm for ^{1}H and 39.5 ppm for ^{13}C relative to TMS. Elemental analysis was provided by Atlantic Microlab, Norcross, GA.

Reaction of 2-Bu$_4$N with Alkyl Halides. General Procedure. The Bu$_4$N salt of nitrosourethane **2-Bu$_4$N** (25 mg, 0.07 mmol) was dissolved in NMR solvent (CD_2Cl_2 or CD_3CN, 0.25 mL) and transferred into an NMR tube. A solution of the alkylation agent (0.07 mmol) in the same solvent (0.25 mL) was added at 0 °C (for MeI and $PhCH_2Br$) or ambient temperature (EtI and *i*-PrI), and the progress of the reaction was monitored by ^{1}H NMR. Characteristic chemical shifts are listed in Table 1.

Thermolysis of the Anion 2 and Kinetic Measurements. Nitrosourethane salt **2-Bu$_4$N** (15 mg) was dissolved in CD_2Cl_2 (0.7 mL) and transferred into an NMR tube. The sample was kept at a constant temperature, and ^{1}H NMR spectra were taken at regular time intervals until almost complete disappearance of the starting material resulted. The ratio of intensities of the signals of the ethyl group quartet in **2** (4.16 ppm) and the butyl group pseudotriplet in Bu_4N^+ (3.22 ppm) was used to calculate the rate constant. The major products of the decomposition of **2** were identified as monoethyl carbonate [**9**: δ 1.12 (t, $J = 7.1$ Hz, 2H) and 3.79 (q, $J = 7.1$ Hz, 2H)] and ethanol [δ 1.17 (t, $J = 7.1$ Hz, 2H) and 3.62 (q, $J = 7.1$ Hz, 2H)].

Thermal Stability of the *O*-Alkyl Derivatives. General Procedure for Kinetic Measurements. The reaction mixtures obtained in CH_2Cl_2 were passed through a silica gel plug to remove the ammonium salts, and the regioisomers were quickly eluted with methylene chloride as one fraction. The solvent was carefully evaporated, and the resulting oily residue of products was dissolved in CD_2Cl_2 (0.5 mL). The solution was kept at 35 °C, and ^{1}H NMR spectra were collected at regular intervals. The ratio of intensities of the signals of the *O*-alkyl methylene group in the starting material (**5b**: 4.56 ppm; **5d**: 5.52 ppm) to that in the *N*-alkyl derivative (**5b**: 3.77 ppm; **5d**: 4.91 ppm) was used to calculate the rate constant. The major products of the decomposition

(58) White, E. H.; DePinto, J. T.; Polito, A. J.; Bauer, I.; Roswell, D. F. *J. Am. Chem. Soc.* **1988**, *110*, 3708—3709.
(59) Yustynyuk, Y. A.; Subbotin, O. A.; Gruzdneva, V. N.; Kazitsyna, L. A. *Dokl. Akad. Nauk* **1976**, *226*, 54—56.
(60) White, E. H.; Dolak, L. A. *J. Am. Chem. Soc.* **1966**, *88*, 3790—3795.
(61) Darbeau, R. W.; Perez, E. V.; Sobieski, J. I.; Rose, W. A.; Yates, M. C.; Boese, B. J.; Darbeau, N. R. *J. Org. Chem.* **2001**, *66*, 5679—5686.
(62) Frisch, M. J.; Trucks, G. W.; Schlegel, H. B.; Scuseria, G. E.; Robb, M. A.; Cheeseman, J. R.; Zakrzewski, V. G.; Montgomery, J. A., Jr.; Stratmann, R. E.; Burant, J. C.; Dapprich, S.; Millam, J. M.; Daniels, A. D.; Kudin, K. N.; Strain, M. C.; Farkas, O.; Tomasi, J.; Barone, V.; Cossi, M.; Cammi, R.; Mennucci, B.; Pomelli, C.; Adamo, C.; Clifford, S.; Ochterski, J.; Petersson, G. A.; Ayala, P. Y.; Cui, Q.; Morokuma, K.; Malick, D. K.; Rabuck, A. D.; Raghavachari, K.; Foresman, J. B.; Cioslowski, J.; Ortiz, J. V.; Stefanov, B. B.; Liu, G.; Liashenko, A.; Piskorz, P.; Komaromi, I.; Gomperts, R.; Martin, R. L.; Fox, D. J.; Keith, T.; Al-Laham, M. A.; Peng, C. Y.; Nanayakkara, A.; Gonzalez, C.; Challacombe, M.; Gill, P. M. W.; Johnson, B. G.; Chen, W.; Wong, M. W.; Andres, J. L.; Head-Gordon, M.; Replogle, E. S.; Pople, J. A. *Gaussian 98*, revision A.9; Gaussian, Inc.: Pittsburgh, PA, 1998.
(63) Scott, A. P.; Radom, L. *J. Phys. Chem.* **1996**, *100*, 16502—16513.
(64) Glendening, E. D.; Reed, A. E.; Carpenter, J. E.; Weinhold, F. *NBO, Version 3.1*.
(65) Clark, T.; Chandrasekhar, J.; Spitznagel, G. W.; Schleyer, P. v. R. *J. Comput. Chem.* **1983**, *4*, 294—301.
(66) Bakhtiar, C.; Smith, E. H. *J. Chem. Soc., Faraday Trans. 1* **1994**, 239—243.

of **5b** and **5d** were identified as diethylcarbonate (**10b**) and benzyl ethylcarbonate (**10d**). For ^{1}H NMR spectral information see Table 1.

Ethyl *N*-Nitrosocarbamate Silver Salt (2-Ag).[8] *N*-Nitrourethane ammonium salt (**6-NH$_4$**, 2.00 g, 13.23 mmol) was dissolved in a mixture of water (30.0 mL) and acetic acid (1.6 mL). Zn dust (1.20 g, 18.35 mmol) was added portionwise at a rate to ensure that the temperature was under 25 °C during the addition (a small amount of ice can be added directly to the reaction mixture if the temperature rises above 30 °C). Stirring was continued for 1 h during which a significant amount of yellow precipitate was formed. Ice was added, followed by aqueous ammonia, in excess. The resultant suspension was stirred for 5 min and filtered through a large filter paper. The filtrate was transferred into a 500 mL Erlenmeyer flask, and ice (100 g) was added, followed by a solution of $AgNO_3$ (2.25 g, 13.23 mmol). Acetic acid was added in small portions to make the solution acidic, causing the formation of a yellow precipitate. The mixture was left standing for 10−15 min, and the resulting solid was filtered and washed successively with water, ethanol, and methanol. The solid was dried in a vacuum at 0 °C to give 1.50 g (50% yield) of the silver salt **2-Ag** as a yellow powder. Anal. Calcd for $C_3H_5AgN_2O_3$: C, 16.02; H, 2.24; N, 12.45. Found: C, 15.74; H, 2.13; N, 11.87.

Ethyl *N*-Nitrosocarbamate Tetrabutylammonium Salt (2-Bu$_4$N). The silver salt **2-Ag** (1.50 g, 6.67 mmol) was suspended in an ice−water mixture, and a solution of Bu_4NBr (2.36 g, 7.34 mmol) was introduced in one portion. The resultant suspension was stirred for 5 min, filtered, and extracted with methylene chloride (5 × 50 mL). The combined organic extracts were dried ($MgSO_4$), and the solvent was removed at 0 °C. Dry ether was added to the resultant yellow solid, and the suspension was stirred for 5 min. The solid material was filtered and dried to give 2.00 g (83% yield based on **2-Ag** or 42% overall yield from **6-NH$_4$**) of **2-Bu$_4$N** as a yellow powder: mp 89−90 °C; ^{1}H NMR (CD_2Cl_2) δ 0.93 (t, J = 7.2 Hz, 12H), 1.27 (t, J = 7.1 Hz, 3H), 1.29−1.41 (m, 8H), 1.52−1.63 (m, 8H), 3.17−3.23 (m, 8H), 4.14 (q, J = 7.1 Hz, 2H); (CD_3CN) δ 0.93 (t, J = 7.2 Hz, 12H), 1.23 (t, J = 7.1 Hz, 3H), 1.25−1.35 (m, 8H), 1.52−1.58 (m, 8H), 3.05−3.10 (m, 8H), 4.08 (q, J = 7.1 Hz, 2H); ^{13}C NMR (CD_2Cl_2) δ 13.7, 15.0, 20.0, 24.3, 59.0, 60.0, 168.0. Anal. Calcd for $C_{19}H_{41}N_3O_3$: C, 63.47; H, 11.49; N, 11.69. Found: C, 62.89; H, 11.72; N, 9.74.

Ethyl *N*-Nitrocarbamate Ammonium Salt (6-NH$_4$).[8] It was prepared in 85% yield according to a literature procedure[32] by nitration of urethane in a KNO_3/H_2SO_4 mixture: mp 165−166 °C dec (lit.[32] 164−165 °C); ^{1}H NMR (DMSO-d_6) δ 1.10 (t, J = 7.1 Hz, 3H), 3.87 (q, J = 7.1 Hz, 2H), 7.16 (bs, 4H); ^{13}C NMR (DMSO-d_6) δ 14.7, 59.3, 160.5.

Ethyl 2-Ethylcarbazate (7). A solution of ethyl carbazate (6.14 g, 59.0 mmol) and acetaldehyde (2.60 g, 59 mmol) in ethanol (50 mL) was stirred at ambient temperature until all aldehyde reacted (about 2 h). Ethanol was evaporated, the semicrystalline white residue was treated with ether, and the ether was evaporated leaving a white solid mixture of carbazone isomers **8**: ^{1}H NMR (CD_2Cl_2) δ isomer A: 1.26 (t, J = 7.2 Hz, 3H), 1.79 (d, J = 5.5 Hz, 3H), 4.15 (q, J = 7.2 Hz, 2H), 6.74 (pseudo d, J = 5.0 Hz, 1H), 8.05 (br s, 1H); isomer B: 1.26 (t, J = 7.2 Hz, 3H), 1.92 (d, J = 5.4 Hz, 3H), 4.18 (q, J = 7.2 Hz, 2H), 7.22 (pseudo d, J = 4.7 Hz, 1H), 8.27 (br s, 1H).

A solution of borane in THF (1.0 M, 62 mL, 62 mmol) was slowly added to the crude solid carbazone at 0 °C. The resulting clear colorless solution was stirred for 20 min and quenched by addition of 10% HCl (30 mL). The biphasic mixture was stirred at 50 °C for 2 h and, when all hydride decomposed, neutralized with solid $NaHCO_3$. Organic products were extracted with ether (3×), dried (Na_2SO_4), and solvent-evaporated. The thick oily residue was dissolved in methylene chloride (20 mL), passed through a silica gel plug (5 cm), and washed with methylene chloride (200 mL). The clear filtrate was evaporated leaving 6.30 g of crude ethyl 2-ethylcarbazate, which was purified by short-path distillation at 80 °C/0.7 mmHg: ^{1}H NMR (CD_2Cl_2) δ 1.04 (t, J = 7.2 Hz, 3H), 1.23 (d, J = 7.1 Hz, 3H), 2.85 (q, J = 7.2 Hz, 2H), 3.4 (br.s, 1H), 4.11 (q, J = 7.1 Hz, 2H), 6.2 (br. s, 1H); ^{13}C NMR (CD_2Cl_2) δ 13.16, 14.96, 46.76, 61.47, 157.95. The compound was used without further purification.

Ethyl 1-Ethylazoxy-2-carboxylate (4b). Solid *m*-chloroperbenzoic acid (85% pure, 1.50 g, 7.4 mmol) was slowly added in small portions to a stirred solution of ethyl 2-ethylcarbazate (**7**, 0.40 g, 3.0 mmol) in methylene chloride (25 mL) at 0 °C. After 4 h the heterogeneous reaction mixture was allowed to warm to ambient temperature, and stirring was continued overnight. After a total of 12 h, the initially developed yellow color of the transient azo compound largely disappeared. The suspension of the acid was filtered off, and pale yellow filtrate was washed with $NaHCO_3$ and dried (Na_2SO_4). The solution was passed through a silica gel plug giving 0.35 g of essentially pure product by TLC. An analytical sample was obtained by column chromatography (CH_2Cl_2/hexanes in 2:1 ratio) as a yellowish oil: ^{1}H NMR (CD_2Cl_2) δ 1.33 (t, J = 7.1 Hz, 3H), 1.54 (t, J = 7.4 Hz, 3H), 4.29 (q, J = 7.4 Hz, 2H), 4.32 (q, J = 7.1 Hz, 2H); (CD_3CN) δ 1.29 (t, J = 7.1 Hz, 3H), 1.48 (t, J = 7.3 Hz, 3H), 4.30 (q, J = 7.1 Hz, 2H), 4.31 (q, J = 7.3 Hz, 2H); ^{13}C NMR (CD_2Cl_2) δ 13.11, 14.33, 64.45, 66.13, 158.20. IR: 1753, 1519, 1221 cm^{-1}. Anal. Calcd for $C_5H_{10}N_2O_3$: C, 41.09; H, 6.90; N, 19.17. Found: C, 41.28; H, 6.91; N, 18.89.

Acknowledgment. We are indebted to Ms. Krystyna K. Kulikiewicz, a visiting graduate student from University of Lodz, Poland, for help with isolation of the azoxy compound **4b**. This project was supported by DARPA/AFOSR F49620-98-1-0483.

Supporting Information Available: Tables of kinetic data, computational results, and ^{1}H NMR spectrum of **2-Bu$_4$N**. This material is available free of charge via the Internet at http://pubs.acs.org.

JA0209058